

## Supplementary Material for “TITLE”

Martí Planasdemunt-Hospital<sup>1,2</sup> and David Oriola<sup>1,2,3</sup>

<sup>1</sup>*Department of Physics, Universitat Politècnica de Catalunya - BarcelonaTech (UPC), 08028 Barcelona, Spain*

<sup>2</sup>*Institute for Research and Innovation in Health (IRIS),  
Universitat Politècnica de Catalunya - BarcelonaTech (UPC)*

<sup>3</sup>*Barcelona Collaboratorium for Modelling and Predictive Biology, 08005 Barcelona, Spain*  
(Dated: March 14, 2025)

In this Supplementary Material, we provide a detailed explanation of the method used to infer mechanical parameters from the fusion experiments. In Section S1, we derive the dynamics of the fusion contact angle  $\theta(t)$  (see Fig. S1) for the case of two proliferating viscoelastic aggregates. Following this, in Section S2 we describe the inference of the model’s dynamical variables and the mechanical parameters from the experimental data.

### S1. CONTINUUM MODEL FOR THE FUSION OF TWO PROLIFERATING MULTICELLULAR AGGREGATES

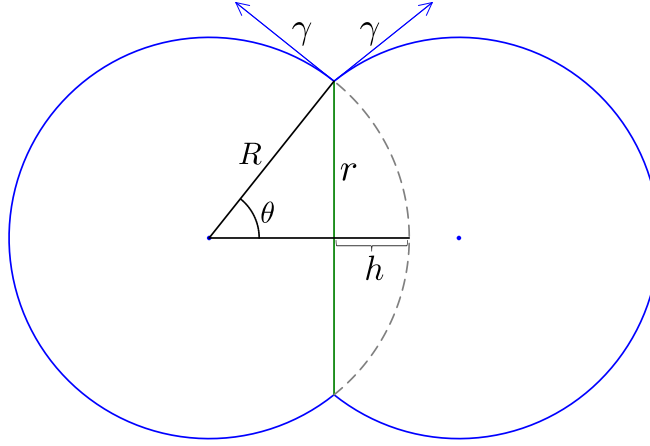


Figure S1: Schematics of the aggregate geometry during fusion. The radius of each fused aggregate  $R$  changes over time due to cell proliferation. The contact angle  $\theta$  describes the degree of fusion in the model. The two aggregates are assumed to have an effective surface tension  $\gamma$  that drives the fusion process. Arrows indicate the direction of the surface tension forces at the confluence. Finally,  $r$  and  $h$  are geometrical parameters.

We consider the fusion of two viscoelastic drops that behave as Kelvin-Voigt materials with effective viscosity  $\eta$  and elasticity  $\mu$ . In addition, the drops have an effective surface tension  $\gamma$  that drives the coalescence process. This description has been shown to be successful in recapitulating the fusion of mouse ES cell aggregates [1] and the derivation of the contact angle dynamics  $\theta(t)$  can be found in Refs. [1, 2]. Here we extend the previous work by considering that the multicellular aggregates proliferate during fusion.

#### A. Surface growth law for proliferating spheroids

Motivated by the linear growth in radius observed for gastruloids from 24 to 48 hpa (see Fig. S2), we consider the following growth law for a single aggregate [1, 3]:

$$\dot{V}_{\text{sphere}} = \Gamma V_c \quad (\text{S1})$$

The previous growth law implies that cells only proliferate in an external spherical crust of constant thickness  $d$  and volume  $V_c$  at a rate  $\Gamma$ , while the rest of the spheroid does not proliferate. It can be easily shown that this law gives rise to a linear increase

on the radius of the spheroid [3]. We define the time-dependent radius of a single aggregate as  $R_0(t) \equiv R_{0,t}$ . The volume of a spherical crust of thickness  $d$  and radius  $R_{0,t}$  reads [3]:

$$V_c(t) = \frac{4}{3}\pi R_{0,t}^3 (3\zeta - 3\zeta^2 + \zeta^3) \quad (\text{S2})$$

where  $\zeta(t) \equiv d/R_{0,t}$  is the relative thickness of the crust compared to the radius of the aggregate. Considering that the crust is thin compared to the sphere radius ( $\zeta(t) \ll 1$ ), we approximate the volume crust to first order in  $\zeta$  such that:

$$V_c(t) \approx 4\pi R_{0,t}^2 d. \quad (\text{S3})$$

As for the volume derivative of the whole sphere containing the crust,  $\dot{V}_{\text{sphere}} = 4\pi R_{0,t}^2 \dot{R}_{0,t}$ . Using the previous result and Eq. (S3), we obtain  $\dot{R}_{0,t} = \Gamma d$ , which yields a linear increase in the radius of the aggregate at rate  $\Gamma$ . Hence, the time evolution of the radius simply reads:

$$R_{0,t} = R_0 + \Gamma d t, \quad (\text{S4})$$

where  $R_0 = R_{0,0} \equiv R_0(t=0)$  and  $\Gamma d$  is the spheroid growth velocity. The previous linear expression is fitted to the time-lapse images of single growing gastruloids from 24 to 48 hpa (see Fig. S2) and the growth velocity  $\Gamma d$  as well as the initial radius  $R_0$  are inferred for the different conditions.

### B. Note on surface growth and the divergence of the velocity field for a single spheroid

Next, we show that surface growth is consistent with the trace of the strain rate tensor being zero everywhere except in the outer crust of thickness  $d$ . We define the strain rate tensor of the spheroid as  $\dot{\epsilon}_0$ . Its trace  $\text{Tr}(\dot{\epsilon}_0)$  corresponds to the divergence of the velocity field. For the special case of surface growth we define the trace of the strain rate tensor as:

$$\text{Tr}(\dot{\epsilon}_0) = \nabla \cdot \mathbf{v} = \Gamma d \delta(r - R_{0,t}(t)) \quad (\text{S5})$$

where  $\delta(r - R_{0,t}(t))$  is a Dirac delta distribution centred at the radial distance  $R_{0,t}(t)$ . We can check the consistency of the previous expression by calculating the flux across the surface of the spheroid, which we denote  $I$ , in two different ways:

$$I = \int_V \nabla \cdot \mathbf{v} dV = 4\pi \int_0^{R_{0,t}(t)} r^2 \Gamma d \delta(r - R_{0,t}(t)) dr = 4\pi \Gamma d R_{0,t}^2(t) \quad (\text{S6})$$

and, by the divergence theorem,

$$I = \int_S \mathbf{v} \cdot \mathbf{n} dS = \dot{R}_{0,t} 4\pi R_{0,t}^2(t), \quad (\text{S7})$$

where  $\mathbf{n}$  is the outward normal vector on the surface of the spheroid and we used  $\mathbf{v} = \dot{R}_{0,t} \mathbf{n}$ . Equating Eqs. (S6) and (S7), we recover the linear growth of the radius  $\dot{R}_{0,t} = \Gamma d$ .

### C. Considerations on the choice of the strain of the assembly

We consider the following expression for the strain that builds up during fusion in the assembly:

$$\varepsilon(R, \theta) = 1 - \frac{R}{2R_{0,t}} (1 + \cos \theta). \quad (\text{S8})$$

where  $R(t)$  corresponds to the radius of each fused aggregate (see Fig. S1) as opposed to the radius of a single aggregate  $R_{0,t}$ . The latter definition assumes that strain in the tissue is only induced by the fusion process and not by the growth of the spheroid. In fact, given that proliferation only occurs at the crust of each single spheroid, it does not yield strain nor pressure gradients in the bulk [4], but only leads to an increase in volume. Thus our strain definition in Eq. (S8) is an extension to the non-proliferating

case, and as such recovers the choice of strain for the non-proliferating case [1] when the growth velocity  $\Gamma d$  is zero. Given the geometry of the problem, the strain tensor  $\varepsilon$  along the axis of fusion is written as (see Refs. [1, 2]):

$$\varepsilon = -\varepsilon(R, \theta) \begin{pmatrix} 1 & 0 & 0 \\ 0 & -1/2 & 0 \\ 0 & 0 & -1/2 \end{pmatrix}, \quad (\text{S9})$$

where we use a traceless tensor given that proliferation is only restricted on the outer crust. Finally, The strain rate along the axis of fusion  $\dot{\varepsilon}$  can be easily computed leading to:

$$\dot{\varepsilon}(R, \theta) = -\frac{1}{2} \left[ \frac{1}{R_{0,t}} \left( \dot{R} (1 + \cos \theta) - R \sin \theta \dot{\theta} \right) - \frac{R \Gamma d}{R_{0,t}^2} (1 + \cos \theta) \right]. \quad (\text{S10})$$

#### D. Derivation of the contact angle dynamics

To derive the contact angle dynamics during fusion, we use Onsager's variational principle [5, 6] in a terminology established by Doi [7] to the fusion of two proliferating viscoelastic drops. Such an approach consists on the minimization of a *Rayleighian* function [8]:

$$\mathcal{R} = \mathcal{D} + \dot{\mathcal{F}} + p\mathcal{Q}. \quad (\text{S11})$$

where  $\mathcal{F}$  is the free energy of the system,  $\mathcal{D}$  is the dissipation term of the assembly,  $\mathcal{Q}$  is a constraint in the system and  $p$  is a Lagrange multiplier that ensures this constraint. In order to evaluate the different terms, we consider an axisymmetric geometry. The dissipation term reads:

$$\begin{aligned} \mathcal{D} &= \eta \int_{\Omega} \dot{\varepsilon} : \dot{\varepsilon} dV = \frac{3}{2} \eta \dot{\varepsilon}^2 \int_{\Omega} dV = \frac{3}{2} \eta \dot{\varepsilon}^2 2 \left( \frac{4}{3} \pi R^3 - \int_0^{R(1-\cos \theta)} \pi r(h)^2 dh \right) = \\ &= \frac{3}{2} \eta \dot{\varepsilon}^2 2 \frac{4}{3} \pi R^3 \left( 1 - (2 + \cos \theta) \sin^4 \frac{\theta}{2} \right) = 4\pi \eta R^3 \dot{\varepsilon}^2 (2 - \cos \theta) \cos^4 \frac{\theta}{2} \end{aligned} \quad (\text{S12})$$

where the symbol  $:$  stands for the inner product between the strain rate tensors. Notice that  $\dot{\varepsilon}(R, \theta)$  from Eq. (S10) is homogeneous in the volume domain  $\Omega$ , provided a given geometry  $(R, \theta)$ . To compute the integral, we used the fact that  $r(h)^2 = R^2 - (R \cos \theta + h)^2$ , which stems from geometrical considerations (see Fig. S1). The free energy  $\mathcal{F} = \mathcal{F}_b + \mathcal{F}_s$  consists of bulk  $\mathcal{F}_b$  and surface  $\mathcal{F}_s$  terms:

$$\mathcal{F}_b = \mu \int_{\Omega} \varepsilon : \varepsilon dV = 4\pi \mu R^3 \varepsilon^2 (2 - \cos \theta) \cos^4 \frac{\theta}{2}, \quad (\text{S13})$$

$$\mathcal{F}_s = \gamma \int_{\partial\Omega} dS = 2\gamma \left( 4\pi R^2 - 2\pi \int_0^{R(1-\cos \theta)} r(h) \sqrt{1 + \left( \frac{dr(h)}{dh} \right)^2} dh \right) = 4\pi \gamma R^2 (1 + \cos \theta). \quad (\text{S14})$$

The constraint  $\mathcal{Q}$  will ensure that the volume of the assembly grows following Eq. S1, that is at each time  $t$ , the volume of the assembly corresponds to  $2V_{\text{sphere}}$ . In other words, the volume increase of each spheroid should be the same regardless of the fusion process. We impose the latter constraint in the system by defining  $\mathcal{Q}$  as:

$$\mathcal{Q} = \dot{V}_{\text{sphere}} - \dot{V}_{\text{fused}}, \quad (\text{S15})$$

where  $V_{\text{sphere}} = 4/3 \pi R_{0,t}^3$  is the previously introduced volume of a single proliferating spheroid of radius (S4) and  $V_{\text{fused}} = 4/3 \pi R^3 (2 - \cos \theta) \cos^4 (\theta/2)$  is the volume of each spheroid during fusion, as shown in Figure S1, which has already been computed in the terms of energy dissipation and bulk free energy (see Eqs. (S12), (S13), respectively). The Lagrange multiplier  $p$  plays the role of the pressure inside the assembly.

Once the *Rayleighian* is defined we apply Onsager's variational principle, which states that the system evolves such that the latter function is minimized with respect to the rate of change of the variables,  $\dot{R}$  and  $\dot{\theta}$ , subject to the constraint  $\mathcal{Q} = 0$ . We find  $\dot{R}$ ,  $\dot{\theta}$  and  $p$  as solutions to the system of equations:

$$\frac{\partial \mathcal{R}}{\partial \dot{R}} = \frac{\partial \mathcal{R}}{\partial \dot{\theta}} = \frac{\partial \mathcal{R}}{\partial p} = 0, \quad (\text{S16})$$

which read

$$\tau \frac{\dot{R}}{R_0} = (\beta - \xi_t) \chi_- \frac{R}{R_0} - 2\beta \frac{R_{0,t}}{R_0} \tan^2(\theta/2) - \left( \frac{R_{0,t}}{R} \right)^2 \frac{\sec^6(\theta/2)}{4(1 + \chi_-)} [2 - 3\xi_0 - (2 + \xi_0)(2\chi_- \cos \theta + 1)], \quad (\text{S17})$$

$$\tau \dot{\theta} = \csc \theta \left( \frac{R_{0,t}}{R} \right)^3 \left[ \left( 2 \frac{R_0}{R_{0,t}} \cos \theta + \xi_t \chi_+ \right) \sec^4(\theta/2) - \left( \frac{R}{R_{0,t}} \right)^2 (1 + \chi_-) \left( 2\beta + \frac{R}{R_{0,t}} (\xi_t - \beta) \chi_+ \right) \right], \quad (\text{S18})$$

$$p = \frac{4\gamma}{R\chi_+} + \frac{3\mu}{4} \left( -2 + \chi_+ \frac{R}{R_{0,t}} \right)^2, \quad (\text{S19})$$

where  $\xi_t = \Gamma d\tau/R_{0,t}$  is a measure of the relative increase in radius in a characteristic fusion timescale  $\tau = \eta R_0/\gamma$ ,  $\beta = \mu R_0/\gamma$  is a dimensionless elastocapillary parameter which characterizes the degree of fusion and  $\chi_{\pm} = 1 \pm \cos \theta$ .

### E. Limit of no spheroid growth

In the limit of no proliferation ( $\xi_t = \xi_0 = 0$ ,  $R_{0,t} = R_0$ ), Eq. (S18) reduces to:

$$\dot{\theta} = \frac{2 - \cos \theta}{\tau \sin \theta} \left[ \beta \left( 1 + \cos \theta - \frac{2R_0}{R(\theta)} \right) + 2 \cos \theta \right], \quad (\text{S20})$$

with,

$$R(\theta) = R_0 2^{2/3} (1 + \cos \theta)^{-2/3} (2 - \cos \theta)^{-1/3}, \quad (\text{S21})$$

which corresponds to the contact angle dependence of the radius of the aggregates during fusion in the incompressible limit [1, 2]. In the same limit, combining Eqs. S20 and S17 one can show that:

$$\dot{R}(\theta) = R(\theta) \frac{(1 - \cos \theta)^2}{(2 - \cos \theta) \sin \theta} \dot{\theta} \quad (\text{S22})$$

The previous expression corresponds to the time derivative of Eq. S21 and therefore we also recover the incompressible dynamics of  $R$ . Finally, if in addition to no growth we also consider the limit of small  $\theta$ , Laplace's law is recovered in Eq. (S19).

## S2. INFERENCE OF MATERIAL PROPERTIES FROM FUSION ASSAYS

The coalescence and growth of 24h gastruloids was studied for three different conditions (gastruloids formed with cells cultured in ESL, 1i or a2i media). The analyzed data corresponded to brightfield snapshots of the fusion process acquired every 10 minutes with pixel size  $0.5979 \mu\text{m}$ . The experiments either involved single-growing gastruloids or the fusion of gastruloid pairs. The software `MORgAna` [9] was used for segmentation and feature extraction, such as area and major axis length. Images were straightened before the analysis to better reproduce the geometry in our model (Fig. S1). The growth velocity  $\Gamma d$  was fitted from the single gastruloid timelapse imaging (24 to 48 hpa) and the mechanical parameters ( $\beta$  and  $\tau$ ) were fitted using the data from the fusion experiments.

### A. Single gastruloid experiments

The model assumes linear growth in time with velocity  $\Gamma d$  for the radius of each spheroid when isolated. Hence, one should obtain the growth velocity from the evolution of single spherical aggregates. In this case, we compute the mean radius evolution over a set of experiments under the same conditions as:

$$\langle R(t) \rangle = \sqrt{\frac{\langle S(t) \rangle}{\pi}}, \quad (\text{S23})$$

where  $\langle S(t) \rangle = 1/n \sum_{i=1}^n S_i(t)$  is the average focal plane area evolution over experiments and  $S_i(t)$  is the area at each snapshot taken at time  $t$  of the gastruloid of experiment  $i$  obtained with `MORgAna`. The standard deviation was computed as:

$$\sigma_R = \sqrt{\frac{1}{n} \sum_{i=1}^n (R_i(t) - \langle R(t) \rangle)^2}. \quad (\text{S24})$$

Once the curve  $\langle R(t) \rangle$  was obtained by the procedure in Eq. (S23), we fitted a linear function  $y = at + b$  to the data (see Fig. S2) according to the model Eq. (S4) by determining the parameters  $0 < a, b < \infty$  using the Trust Region Reflective method for least squares optimization implemented by the function `curve_fit` of the `optimize` submodule in SciPy. After this procedure,  $\Gamma d = a$  was inferred from the data.

### B. Fusion experiments

Once the growth velocity  $\Gamma d$  was known for a given condition,  $\beta$  and  $\tau$  were obtained for that same condition from the fusion experiments. For that, we first inferred the mean sine squared of the fusion angle evolution over the set of experiments,

$$\langle \sin^2 \theta(t) \rangle = \frac{1}{n} \sum_{i=1}^n \sin^2 \theta_i(t). \quad (\text{S25})$$

Each  $\theta_i(t)$  is the solution to the transcendental equation

$$L_i(t) = 2R_i(\theta_i(t), t)(1 + \cos \theta_i(t)) \quad (\text{S26})$$

for each experiment  $i$ , where  $L_i(t)$  is the major axis length, obtained as data by `MORgAna`, and the expression  $R_i(\theta_i(t), t)$  is derived from the volume conservation during fusion equation  $\partial \mathcal{R} / \partial p = 0$  integrated over time:

$$R_i(\theta_i(t), t) = R_{0,t}(2 - \cos \theta_i(t))^{-1/3} \cos(\theta_i(t)/2)^{-4/3}. \quad (\text{S27})$$

The standard deviation is computed as

$$\sigma_{\sin^2 \theta(t)} = \sqrt{\frac{1}{n} \sum_{i=1}^n (\sin^2 \theta_i(t) - \langle \sin^2 \theta(t) \rangle)^2}. \quad (\text{S28})$$

For the fitting procedure, we again used the same `curve_fit` function with the  $\langle \sin^2 \theta(t) \rangle$  data curve Eq. (S25) and found the optimal parameters  $\beta$  and  $\tau$  for the solution of the ODE (S18) plugged into a sine squared, which is now the fitting function. The initial radius of an aggregate  $R_0$  in Eq. (S17)-(S18) was taken as  $R_0 = \langle L_i(0) \rangle / 4$ .

### C. Error treatment

Each fitted parameter value has its standard deviation, properly propagated in terms of the inferred quantities. The `curve_fit` function outputs the covariance matrix, whose diagonal elements are the variance of each fitted parameter. For the first fit to a line in the single-spheroid radius evolution (Fig. S2), we computed the coefficient of determination

$$r^2 = 1 - \frac{\sum_j (\langle R(t_j) \rangle - R_{0,t}(t_j))^2}{\sum_j (\langle R(t_j) \rangle - \overline{\langle R(t_j) \rangle})^2}, \quad (\text{S29})$$

where  $j = 0, \dots, N$  spans the time window of the available snapshots and  $\overline{\langle R(t_j) \rangle}$  is the time average of the data Eq. (S23). For the second fit of the degree-of-fusion evolution, we computed the Root Mean Square Error

$$RMSE = \sqrt{\langle (\sin^2 \theta(t) - y(t))^2 \rangle} \quad (\text{S30})$$

where  $y(t)$  is the sine squared of the solution of Eq. (S18) for the optimal parameters found.

- [2] S. Samatas, M. Planasdemunt-Hospital, and D. Oriola, *Biophysica* **4**, 604 (2024).
- [3] A. D. Conger and M. C. Ziskin, *Cancer Research* **43**, 556 (1983).
- [4] B. I. Shraiman, *Proceedings of the National Academy of Sciences* **102**, 3318 (2005).
- [5] L. Onsager, *Physical review* **37**, 405 (1931).
- [6] L. Onsager, *Physical review* **38**, 2265 (1931).
- [7] M. Doi, *Journal of Physics: Condensed Matter* **23**, 284118 (2011).
- [8] M. Arroyo, N. Walani, A. Torres-Sánchez, and D. Kaurin, *The role of mechanics in the study of lipid bilayers*, 287 (2018).
- [9] N. Gritti, J. L. Lim, K. AnlaÅ, M. Pandya, G. Aalderink, G. MartÁnez-Ara, and V. Trivedi, *Development* **148**, dev199611 (2021), <https://journals.biologists.com/dev/article-pdf/148/18/dev199611/2103461/dev199611.pdf>.

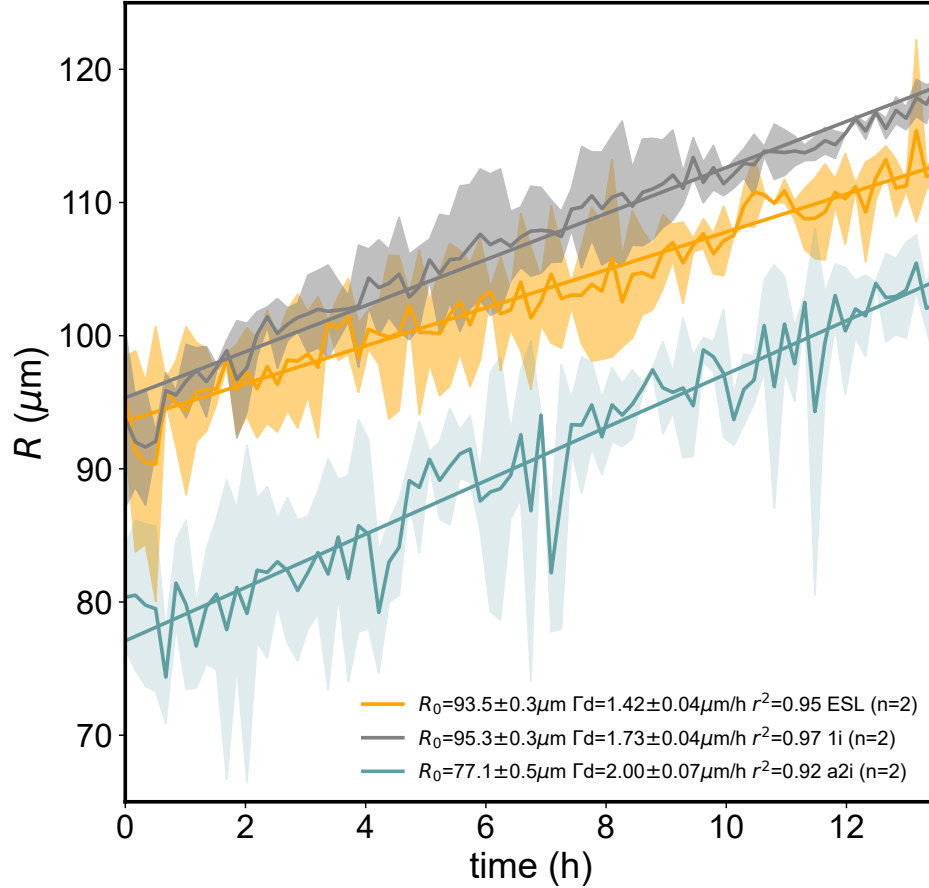


Figure S2: Inferred radius evolution from  $n = 2$  experiments of every condition ESL, 1i and a2i. Rough lines are the average over experiments and the shadowed regions around them show the bounds at one standard deviation distance. Straight lines result from the fitting for each colour. The legend contains the values of the fitted parameters of the Equation (S4) together with its standard deviation and the coefficient of determination  $r^2$ . For this fit, only the  $\Gamma d$  value is used for the fusion dynamics, since the initial radius is inferred from the fusion experiments according to  $R_0 = \langle L_i(0)/4 \rangle$ .